JOURNAL OF AIRCRAFT
Vol. 46, No. 5, September–October 2009

Modeling Pilot Control Behavior with Sudden Changes in Vehicle Dynamics

Ronald A. Hess*
University of California, Davis, Davis, California 95616-5294

DOI: 10.2514/1.41215

A pursuit tracking model of the human pilot adapting to sudden changes in vehicle dynamics is developed and exercised. The current model is based upon a simplified representation of the human pilot in multi-axis tasks previously reported in the literature. A key feature of the adaptive model is the simplicity afforded by only varying two gain parameters in each control loop to accommodate pilot adaptation. The model is first exercised in a single-loop task in which the controlled element dynamics are changed from rate command to acceleration command (with time delay), back to rate command, and finally, to position command. A second example applies the model to a simple two-axis task (two control inceptors) in which the controlled element dynamics in both control loops are changed simultaneously. The model employed for sudden changes in vehicle dynamics is also applied to a single-axis task in which the controlled element dynamics change gradually over a 10 s period. Finally, longitudinal control of a simplified model of a fighter aircraft undergoing sudden damage is considered.

Nomenclature

C	=	command to position feedback loop in pilot model
CF1, CF2	=	transfer functions of cross-coupling dynamics in two-axis tracking example
f	=	task interference parameter in two-axis application of pilot model
G_{nm}	=	model of the pilot's neuromuscular system
K_p	=	"position" feedback gain in pilot model
K_r	=	"rate" feedback gain in pilot model
K_{trigger}	=	trigger parameter in pilot model adaptation law
M, $\dot{M}$	=	controlled element output and output rate
R	=	command to rate feedback loop in pilot model
t_c	=	"criteria time" at which controlled element dynamics change
x	=	signal in pilot model adaptation law
Y_c	=	controlled element transfer function
δ	=	pilot control input

Introduction

INTEREST in modeling the adaptive characteristics of the human operator/pilot began over five decades ago and continued into the mid-1970s, for example, [1–17]. Although interest waned in the intervening years, it has been rekindled by recent research in adaptive and reconfigurable flight control systems, for example, [18]. This renewed interest is attributable to questions that have arisen as to the ability of the human pilot to adapt to changing vehicle dynamics during and after the reconfiguration process. The research to be summarized has, as its goal, the development of a simple model for human pilot adaptation and the application of this model to a pair of control tasks in which sudden and significant changes in control system dynamics occur. A review of the research described in [1–17] is beyond the scope of this discussion. Such a review would, for the most part, merely echo the excellent summary provided in [13]. In contrast to these earlier modeling efforts, the approach to be discussed herein builds upon a simplified pursuit control model of the pilot that has been used in assessing degraded visual cues and vehicle handling qualities [19]. As such, the model is an extension of an existing structure that has been successfully used to describe human pilot control behavior in the absence of changing vehicle dynamics.

Received 24 September 2008; revision received 8 June 2009; accepted for publication 18 June 2009.

*Professor, Department of Mechanical and Aeronautical Engineering. Associate Fellow AIAA.

Background

The research summarized in [19] presents a control-theoretic procedure for modeling human pilot pursuit control behavior for flight control applications. Here "pursuit" refers to scenarios in which the human can discern system output from input, that is, more than just "error" information is available to the pilot. Figure 1 shows the model for a single-axis tracking task. Only two variables parameterize the model, the gains K_r and K_p, respectively, in the rate (r) and position (p) loops. The element G_{nm} in Fig. 1 represents a second-order model of the pilot's neuromuscular system,

$$G_{\text{nm}} = \frac{10^2}{s^2 + 2(0.707)10s + 10^2} \tag{1}$$

Because of the manner in which the gain K_r is selected, the particular units on G_{nm} are of no consequence in the modeling procedure.

Table 1 shows values of K_r and K_p that yielded pilot models that conformed to the "crossover model" of the human pilot [20] for the variety of controlled elements indicated. The last element represents the "limits of manual" control for the pilot model in question. Figure 2 shows the resulting open-loop Bode plots demonstrating the crossover-model characteristics. The methods for selecting K_r and K_p are outlined in [19] and are based upon simple frequency-domain procedures. Hess [19] also demonstrates application of the model to multi-axis flight tasks. Hess [21] also demonstrates how these gains can also be selected from nonlinear simulation models of the vehicle being controlled.

It should be noted that the model of Fig. 1 and [19] differs from the structural pilot model discussed in [22] in a number of ways, but primarily in the absence of a proprioceptive feedback loop. In this light, the model of Fig. 1 involves some simplifications that will become apparent in examining open-loop pilot/vehicle transfer functions.

Adaptive Model

The fundamental hypothesis behind the adaptive model to be discussed is that the primary adaptation of the human pilot to changes in the vehicle dynamics occurs through selection of the inner-loop gain K_r. Changes in the outer-loop gain K_p are hypothesized to provide a vernier adjustment to improve system tracking performance. Changes in K_r are hypothesized to occur through sensed

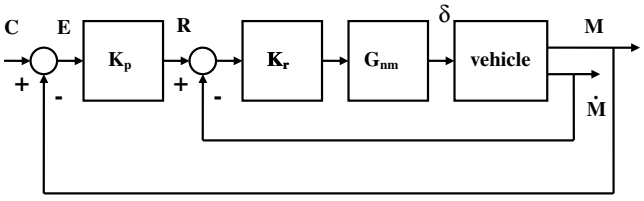

Fig. 1 A simplified pursuit control model of the human pilot [19].

changes in the sign and magnitude of $R - \dot{M}$ in Fig. 1, that is, the error signal in the inner rate loop that occurs when the vehicle dynamics have changed. The basic adaptive relationship that was empirically derived was to increase (decrease) K_r according to the following relations.

Let

$$x = \text{sgn}\{[|R| - |\dot{M}|]\} \cdot [|R| - |\dot{M}|]^2 \cdot \frac{1.5^2}{s^2 + 2(1.5)s + 1.5^2} \tag{2}$$

and

$$t_c = \text{time of failure initiation} \tag{3}$$

$$K_{\text{trigger}} = 0 \text{ if instantaneous value of } |x| < 3 \cdot \text{rms value of } |x| \quad \text{or}$$
$$t < t_c = 1 \text{ if instantaneous value of } |x| \geq 3 \cdot \text{rms value of } |x|$$
$$\text{and} \quad t \geq t_c \tag{4}$$

Then

$$\Delta K_r = x \cdot K_{\text{trigger}} \tag{5}$$

The gain K_p was changed according to the relations

$$\begin{aligned} \Delta K_p &= 0.35 \cdot \Delta K_r \quad \text{if } \Delta K_r > 0 \\ &= 0 \qquad\qquad\ \ \text{if } \Delta K_r \leq 0 \end{aligned} \tag{6}$$

The "criteria time" t_c, that is, the time in the simulation run when the controlled element dynamics changed, was chosen after the rms value of x had reached an asymptotic value, mimicking somewhat, the human's ability to recognize nominal system performance. A factor of 3 was chosen in Eqs. (4) as it would represent an instantaneous "3-σ" value. Obviously, too small a trigger value would cause normal system disturbances (e.g., turbulence) to initiate unwanted pilot model adaptation, whereas too large a value would inhibit adaptation when it is needed.

The ad hoc nature of these adaptation laws is obvious. They are based upon the author's experience in choosing gain values for the pursuit model of [19]. The logic summarized in Eqs. (2–6) and the pilot model in which they are to be implemented constitute a candidate framework in which to view, categorize, and summarize pilot behavioral data when vehicle dynamics are subject to sudden changes. The laws were not chosen arbitrarily, however, and are based upon four criteria:

Table 1 Pilot model gain values [19]

Controlled element	K_r	K_p
$\frac{1}{(s^2+2(0.707)5s+25}$	13.5	3.62
$\frac{1}{s(s+10)}$	20.5	2.91
$\frac{1}{s(s+4)}$	11.5	2.56
$\frac{1}{s(s+2)}$	9.19	2.35
$\frac{1}{s^2}$	7.58	1.91
$\frac{0.696(s+0.14)}{s^3+0.424s^2+0.0353s+0.397}$	11.3	1.96
$\frac{1}{s^2(s+11)}$	58.0	1.76

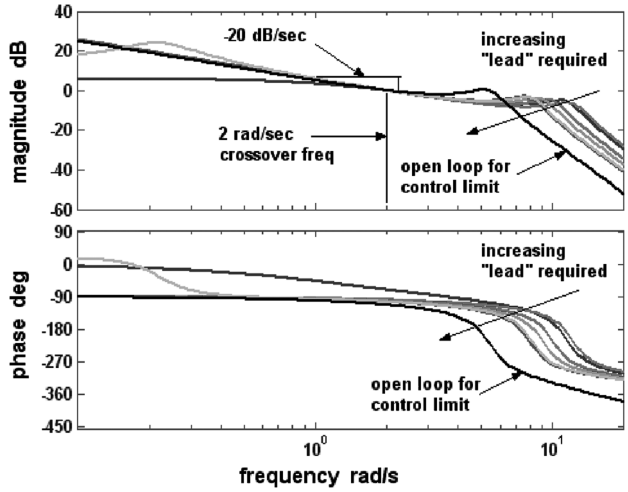

Fig. 2 Bode plots of pilot/vehicle transfer functions for the controlled element dynamics of Table 1 [19].

1) The adjustments to K_r and K_p must be predicated upon observations that can easily be made by the human (under the feedback structure of the model of Fig. 1).

2) The logic driving the adjustments to K_r and K_p must be predicated upon information available to the human.

3) The postadapted pilot models must follow the dictates of the crossover model of the human pilot.

4) Adaptation times must be relatively short and consistent with that obtained in laboratory experiments involving sudden changes in controlled element dynamics, for example, those of [5]. These times were on the order of 5 s.

Figure 3 shows the model of the adaptive human pilot. A limiter is placed at the pilot's inceptor output to model amplitude limitations of the device.

Computer Simulation: Single-Axis Tasks

Figures 4–9 show a series of time histories for system input/output and pilot control input (C, M, and δ in Figs. 1 and 3) as the controlled element dynamics [$Y_c(s)$] were changed as follows in this single-axis task:

$$Y_c(s) = \frac{1}{s(s+10)} \Rightarrow \frac{e^{-0.025s}}{s^2} \Rightarrow \frac{1}{s(s+10)} \Rightarrow \frac{1}{s+50} \tag{7}$$

In implementing the controlled elements in the computer simulations to follow, the needed rate information ($\dot{M}$) was always created by including an integrator just before the output variable (M) was defined and using the input to that integrator as $\dot{M}$. Thus, if the actual controlled element was $Y_c(s) = 1/(s+50)$, an integrator was placed at the plant output, and an element $s/(s+50)$ was inserted before the integrator. The output of $s/(s+50)$ then defined $\dot{M}$. This process obviated pure time differentiation to obtain $\dot{M}$ in the computer simulations which was found to be destabilizing. The command input in the task was selected as a series of pulses, each lasting 5 s. This input was chosen as its simplicity allows a quick appraisal of the tracking performance of the adaptive pilot model. In terms of the classic crossover model of the human pilot [20], the controlled elements of Eq. (7) require pilot equalization that ranges from a pure gain (for $Y_c(s) = 1/[s(s+10)]$), to lead [for $Y_c(s) = e^{-0.025s}/s^2$], to lag [for $Y_c(s) = 1/(s+50)$]. This provides challenging systems for adaptation. In Figs. 8 and 9 the amplitude limits on the control input were increased from ± 50 to ± 150 to allow sufficient control power to be available. Finally, the nominal crossover frequency for the initial simulation ($Y_c(s) = 1/[s(s+10)]$), was set to 1.5 rad/s.

Figure 10 shows the Bode plots for the open-loop pilot/vehicle systems after adaptation. The characteristics of the crossover model are in evidence in each case. The absence of high-frequency

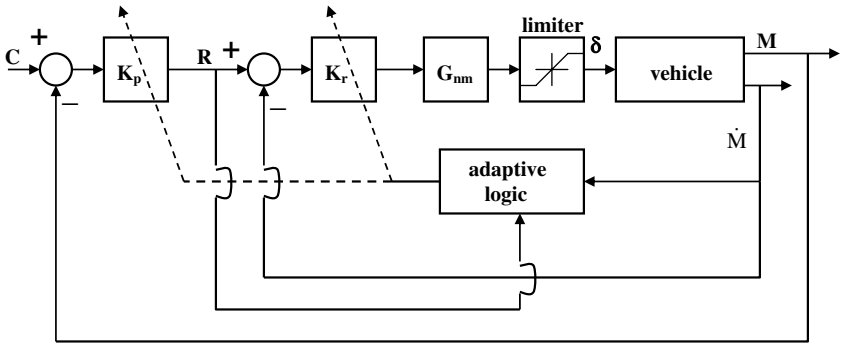

Fig. 3 Model of adaptive human pilot.

amplitude and phase roll-off in one of the bode plots (for the transition of Fig. 8) is attributable to the high-bandwidth nature of the controlled element dynamics. This was not considered to be a serious problem at this juncture. The relatively flat magnitude plot at low frequencies is typical of measured pilot/vehicle transfer functions with controlled element dynamics that resemble a pure gain over a large frequency range, for example, [23]. The crossover frequency for the transition of Fig. 8 is considerably larger than that for either of the other two transitions. This phenomenon has also been noted in crossover-model applications (e.g., [24]), although not to the extent evident in Fig. 10.

Each pair of figures in Figs. 4–9 represents a single computer simulation run. The current adaptive model setup will only allow a single controlled element change per run. Thus, in moving from, say, Figs. 4–7, the simulation was reinitialized with the adapted pilot gains from the runs that yielded Figs. 4 and 5.

Figures 11 and 12 show time histories similar to Figs. 4 and 5 save that a random-appearing input is employed. This one example was included to demonstrate the pilot adaptation is not necessarily input dependent. Control oscillations are evident in Fig. 12, as was the case in Fig. 5. Figure 13 shows the K_r and K_p time histories for this controlled element change. Note no change in K_p was required.

Computer Simulation: Two-Axis Task

For the sake of completeness, a computer simulation of the adaptive model(s) in a two-axis task was undertaken. Here, "two axis" implies that two control inceptors are being used by the pilot to control two response variables. Figure 14 is a Simulink® diagram of the computer simulation for this task.

The nominal controlled element dynamics for each loop are identical, $1/[s(s+4)]$. In addition, control cross coupling is introduced

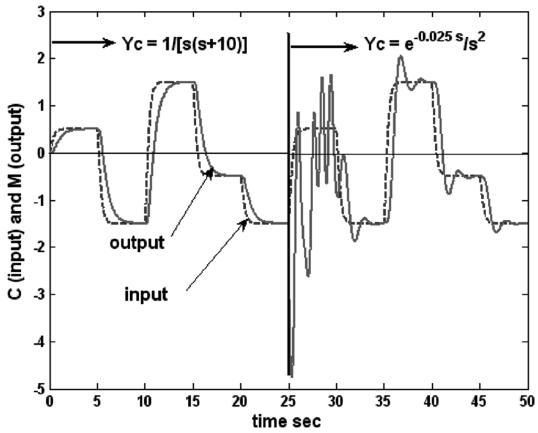

Fig. 4 System input/output time histories for abrupt controlled element change from $Y_c = 1/[s(s+10)]$ to $e^{-0.025s}/s^2$ at $t = 25$ s.

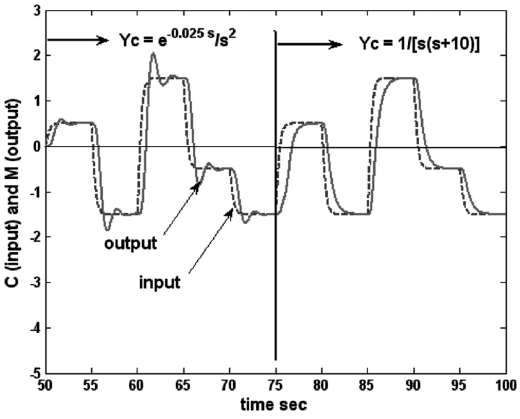

Fig. 6 System input/output time histories for abrupt controlled element change from $Y_c = e^{-0.025s}/s^2$ back to $1/[s(s+10)]$ at $t = 75$ s.

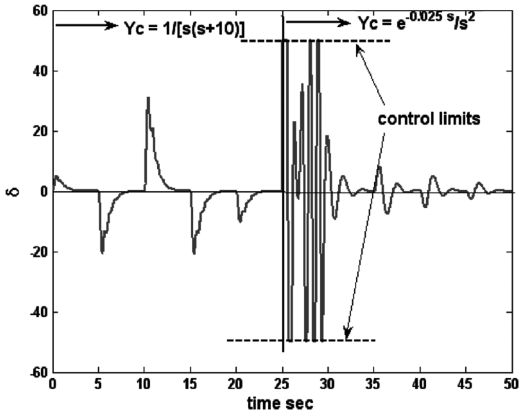

Fig. 5 Pilot control time history for abrupt controlled element change from $Y_c = 1/[s(s+10)]$ back to $e^{-0.025s}/s^2$ at $t = 25$ s.

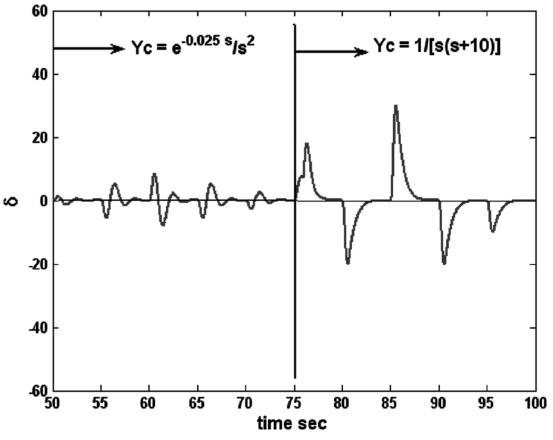

Fig. 7 Pilot control time history for abrupt controlled element change from $Y_c = e^{-0.025s}/s^2$ back to $1/[s(s+10)]$ at $t = 75$ s.

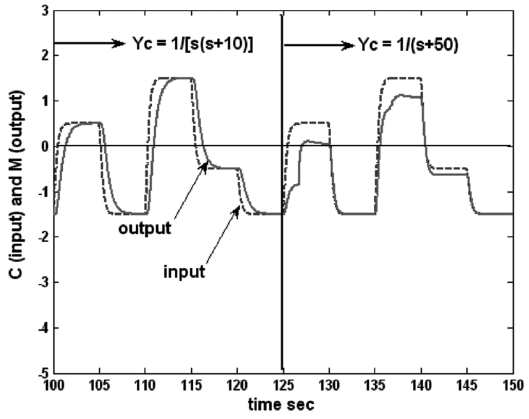

Fig. 8 System input/output time histories for abrupt controlled element change from $Y_c = 1/[s(s + 10)]$ to $1/(s + 50)$ at $t = 125$ s.

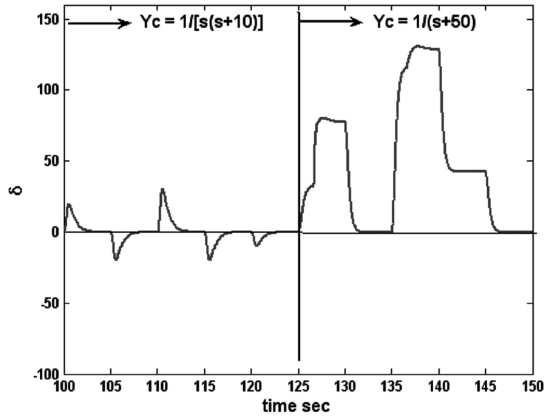

Fig. 9 Pilot control time history for abrupt controlled element change from $Y_c = 1/[s(s + 10)]$ to $1/(s + 50)$ at $t = 125$ s at $t = 75$ s.

between the pilot control inputs for loop 1 (2) and the inputs to the integrators of the controlled element of loop 2 (1). This was done to emulate vehicle dynamics in which such cross coupling is present. The cross-coupling dynamics were chosen as CF1 = CF2= $0.1/(s + 1)$. Random-appearing input commands $C1(t)$ and $C2(t)$ were each generated as sums of seven sinusoids. The nominal pilot model gains were selected from the third row of Table 1, that is, those appropriate for $1/[s(s + 4)]$ controlled element dynamics. In addition, a task interference parameter, introduced in [25] was employed.

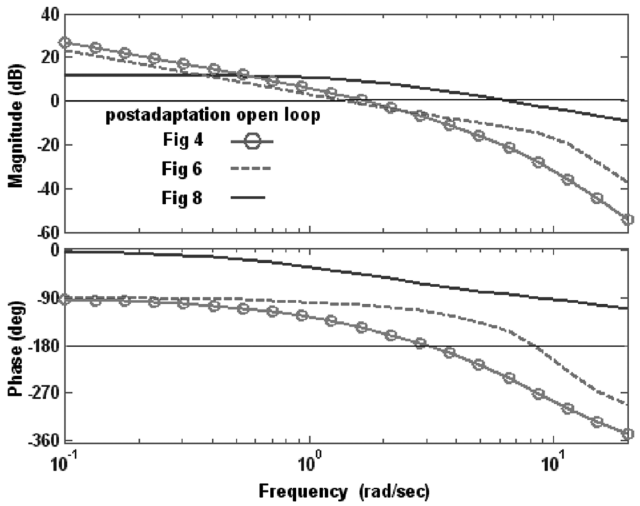

Fig. 10 Bode plots of the open-loop pilot/vehicle systems after adaptation.

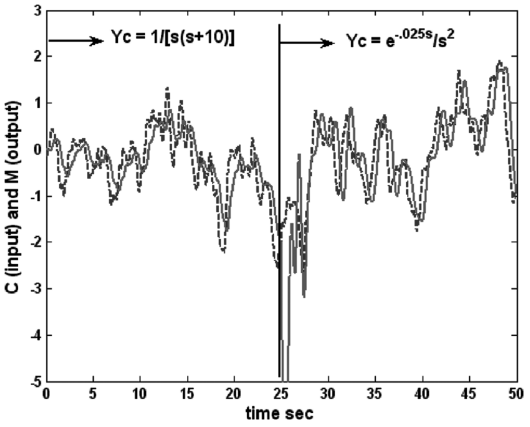

Fig. 11 System input/output time histories for abrupt controlled element change from $Y_c = 1/[s(s + 10)]$ to $e^{-0.025s}/s^2$ at $t = 25$ s, random-appearing input.

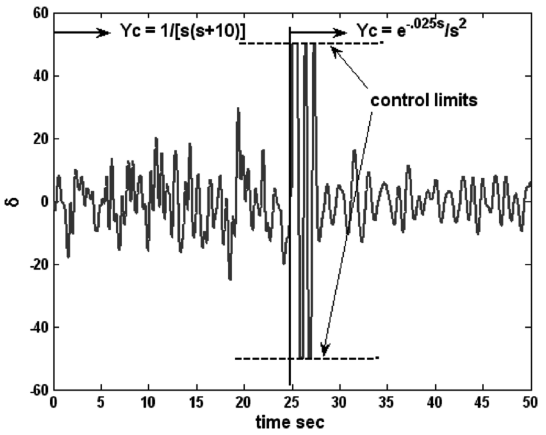

Fig. 12 Pilot control time history for abrupt controlled element change from $Y_c = 1/[s(s + 10)]$ to $e^{-0.025s}/s^2$ at $t = 25$ s, random-appearing input.

Here, this meant changing the single-axis K_r value in Table 1 to K_r/f, where

$$f = 1 + 0.1n \tag{8}$$

where n = no. of axes being controlled by the pilot. Two identical, adaptive pilot models are employed using the same logic as in the single-loop examples, with one addition. A limiter was employed in the adaptive loop for K_r in each pilot model. The limits were applied to the ΔK_r calculations such that

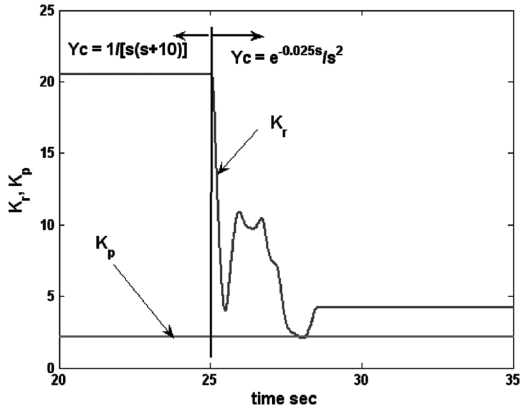

Fig. 13 K_p and K_r time histories for abrupt controlled element change of Figs. 11 and 12.

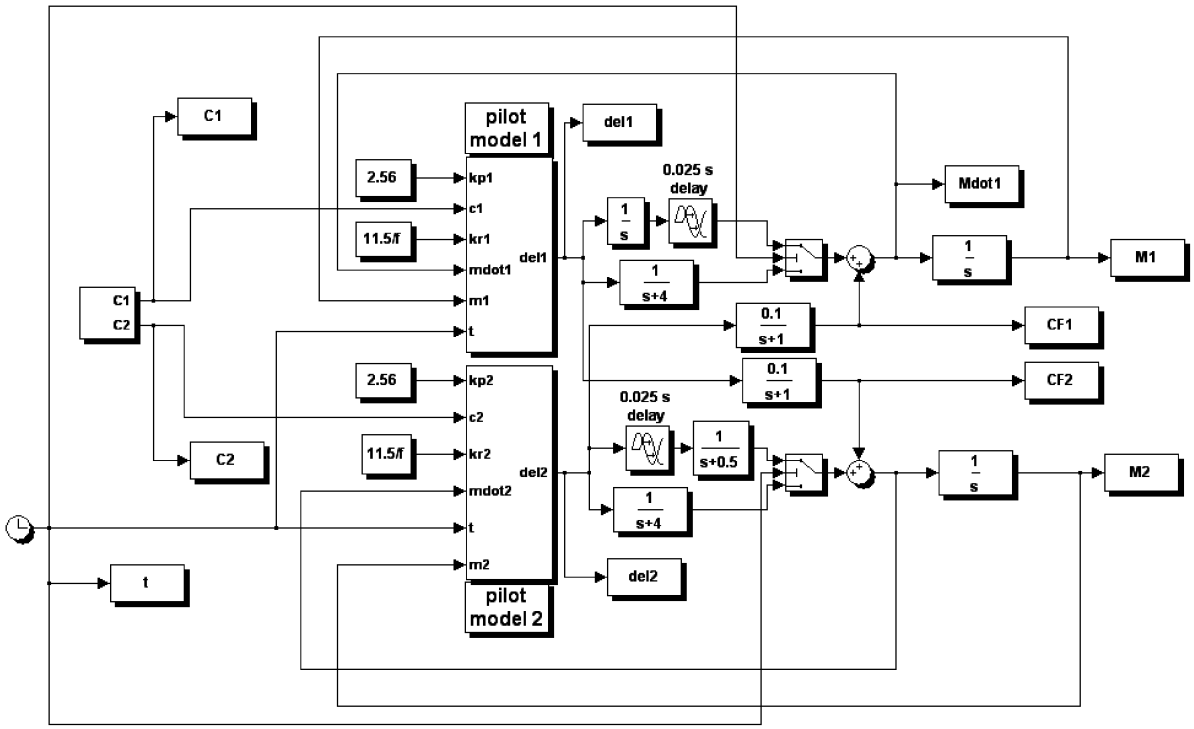

Fig. 14 A Simulink® diagram of the two-axis task.

$$\Delta K_r|_{\max} = \pm 0.5 \cdot [K_r|_{\text{nom}}]/f \tag{9}$$

that is, ±50% of the value of K_r for the pilot model tuned to the nominal controlled element dynamics. The $\Delta K_r|_{\max}$ was also then used in implementing Eq. (6). The modification of Eq. (9) was necessary for the stability of the adaptive pilot model.

Figure 15 shows tracking results for the first control loop in the nominal case. Similar results were apparent for the second control loop. Figure 16 compares the derivative of $M1$ and the cross-feed signal CF1. The latter figure was included to demonstrate that a significant amount of cross coupling was in evidence in the simulation.

Figures 17 and 18 show the tracking results for loops 1 and 2 when the controlled element dynamics of these loops were changed at $t = 52$ s as follows:

$$\text{Loop 1} \quad Y_{c1}(s) = \frac{1}{s(s+4)} \Rightarrow \frac{e^{-0.025s}}{s^2(s+4)}$$
$$\text{Loop 2} \quad Y_{c2}(s) = \frac{1}{s(s+4)} \Rightarrow \frac{e^{-0.025s}}{s(s+0.5)(s+4)} \tag{10}$$

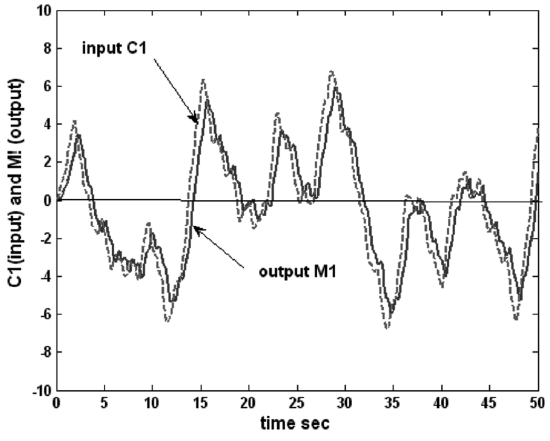

Fig. 15 Tracking results for the first control loop in the nominal case.

Both pilot models adapted to the changed dynamics. As in the single-axis simulations, significant output oscillations are evident in Fig. 17, attributable to the significant degradation in the handling qualities in moving from the nominal to the modified dynamics of the first of Eqs. (10). Finally, when the adaptive capabilities of the pilot models were removed, the system went unstable shortly after the controlled element change at $t = 52$ s.

Computer Simulation: Single-Axis Task with Gradually Changing Dynamics

An additional single-axis example is considered. Rather that an abrupt change in controlled element dynamics, the change occurs over a 10 s period. In an approximate sense, this simulation models what may happen in a reconfigurable control system in which the reconfiguration takes place over a period of seconds, rather than instantaneously. The change in dynamics is identified as

$$Y_c(s) = \frac{1}{s(s+10)} \Rightarrow \frac{e^{-0.05s}}{s(s+5)} \text{ over 10 s period} \tag{11}$$

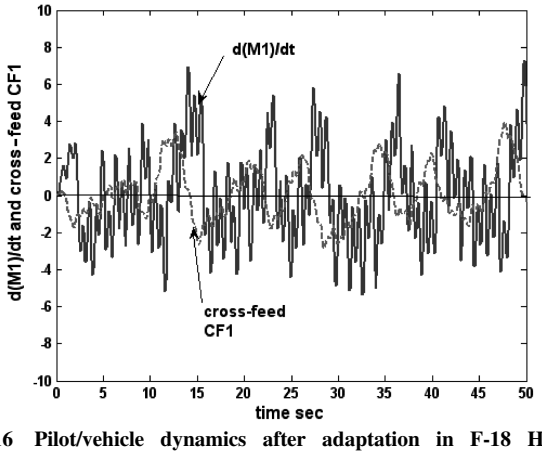

Fig. 16 Pilot/vehicle dynamics after adaptation in F-18 HARV example.

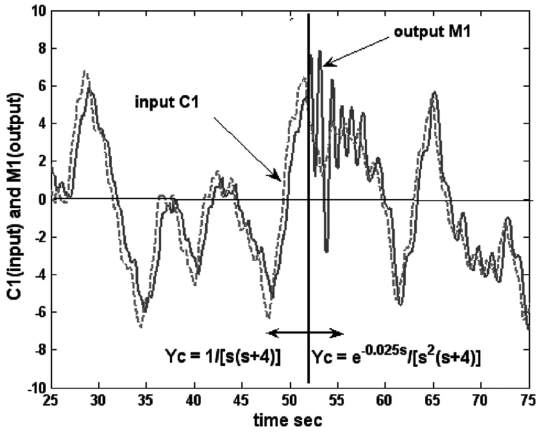

Fig. 17 Tracking results for the first control loop in Fig. 14 for a sudden change in the controlled element dynamics.

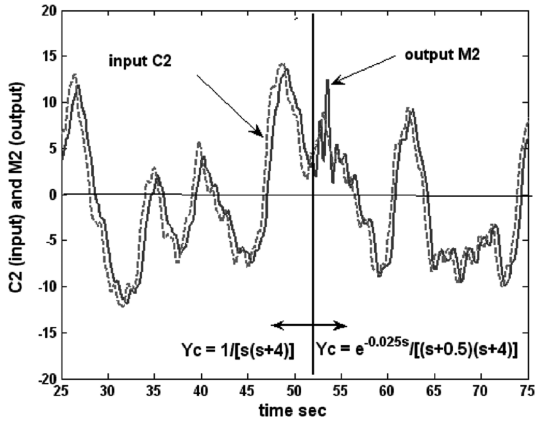

Fig. 18 Tracking results for the second control loop in Fig. 14 for a sudden change in the controlled element dynamics.

The change is implemented in the computer simulation by creating both sets of dynamics and then summing the outputs to the pilot input after they pass through the weighting functions shown in Fig. 19. As the figure indicates, the change was initiated at $t = 30$ s into the run. Again, this time was selected to allow the rms error signals in the pilot/vehicle system to reach asymptotic values with the "healthy" vehicle.

No changes in the adaptive structure of the pilot model were made. The nominal pilot model characteristics were again taken from the second row of Table 1. A random command was applied to the pilot/

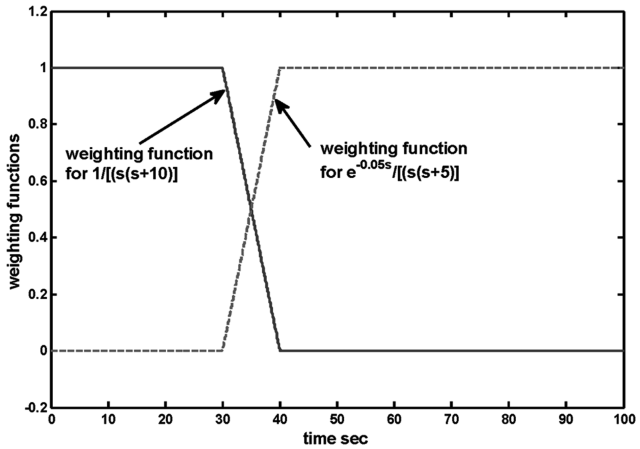

Fig. 19 Weighting functions for implementing gradual (10 s) change in controlled element dynamics.

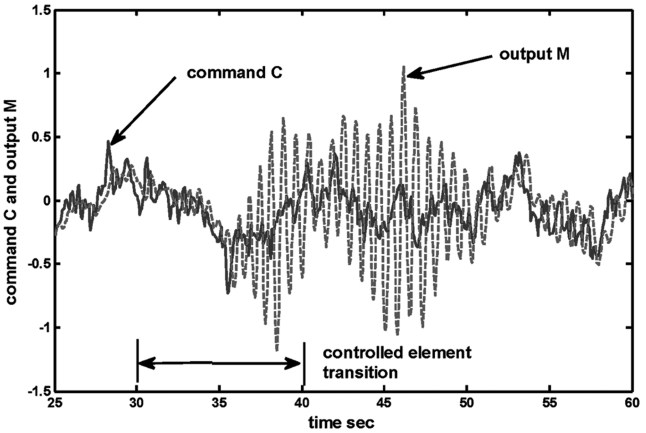

Fig. 20 System input/output time histories for gradual controlled element change from $Yc = 1/([s(s + 10)]$ to $e^{-0.05s}/[s(s + 5)]$, random-appearing input.

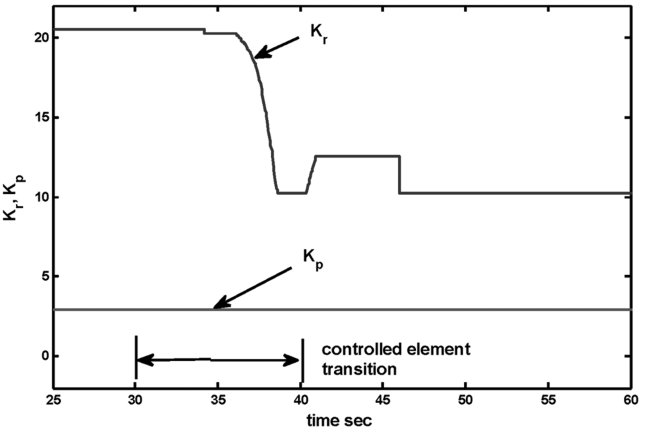

Fig. 21 K_p and K_r time histories for gradual controlled element change.

vehicle system. Figure 20 shows the tracking performance. Significant oscillatory behavior is in evidence for over 10 s. This suggests such a change might be susceptible to a pilot-induced oscillation (PIO). Figure 21 shows the pilot gains K_p and K_r. No K_p change is made. Because the change in controlled element dynamics, itself, takes 10 s to complete, the fact that the pilot model took longer than the "target" 5 s is understandable.

Final Computer Simulation: Single-Axis Task with F-18 HARV

The final computer simulation involved piloted control of a simplified longitudinal model of the F-18 HARV, shown in Fig. 22. This vehicle model has been used in other studies, for example, [26]. Longitudinal control was effected by horizontal stabilator and thrust vectoring inputs. A rate-command stability and command augmentation system was included in the simulation. The tracking task consisted of following a series of pulsive pitch attitude commands. Significant modeled "damage" occurred at $t = 50$ s in a 100-s tracking run. The damage consisted of the following: 1) 50% loss of the horizontal stabilator area, 2) lockup of the horizontal stabilator at -3 deg, 3) a 50% reduction of the thrust vector actuator bandwidth, and 4) the addition of a 0.05-s time delay at the input to each actuator. Figures 23–26 show the simulation results. Improved tracking is seen with pilot adaptation and the pilot/vehicle dynamics after adaptation are seen to exhibit the characteristics of the crossover model.

Discussion

The most critical of the adaptations in the single-axis case for sudden controlled element changes is seen to occur in moving from

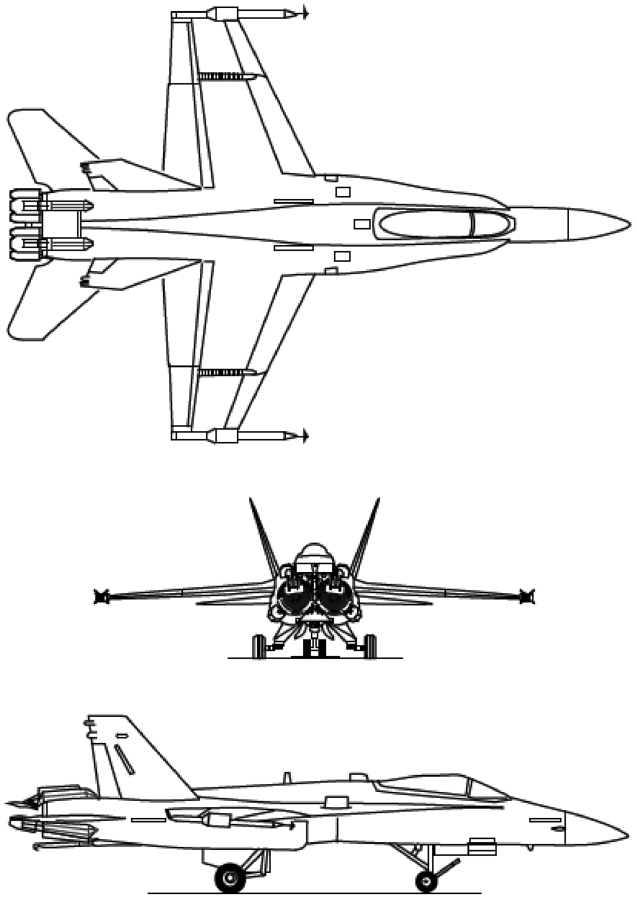

Fig. 22 The F-18 HARV.

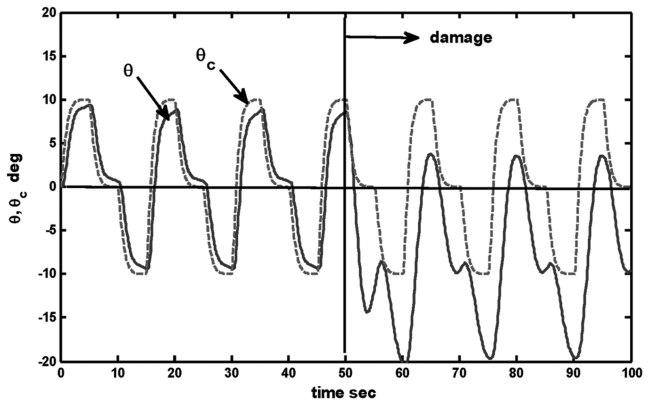

Fig. 23 Tracking results with no pilot model adaptation.

the relatively easy-to-control $Y_c = 1/[s(s + 10)]$ to the very difficult $Y_c = e^{-0.025s}/s^2$. The pilot's inceptor output δ is seen to reach the amplitude limits and a closed-loop oscillation occurs, with both the pulsive and random commands. Were these actual flight control tasks in which rate-limited actuators were in evidence, a sustained PIO could likely have ensued in each case. Each of the pilot adaptations occurred in under 5 s when sudden changes in dynamics were encountered. Without adaptation, pilot/vehicle performance in the controlled element transitions was very poor. The simple multi-axis task simulation suggests that extension of the adaptive model to such tasks is feasible. Again, adaptation occurred within 5 s in the control loops.

Incorporating the modification of Eq. (9) in the computer simulations of the single-axis tasks increased the tracking error from that evident in Fig. 8 (the only example in which changes in K_p occurred)

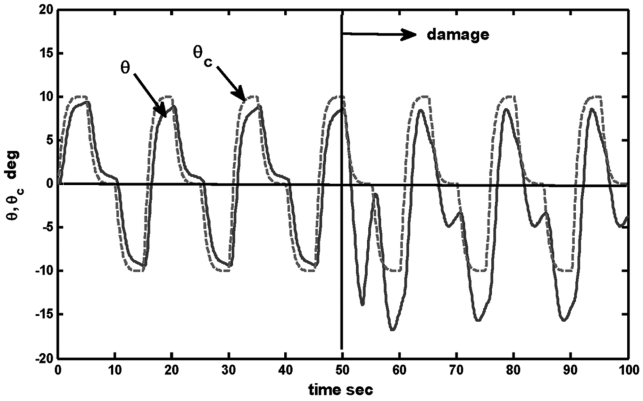

Fig. 24 Tracking results with pilot model adaptation.

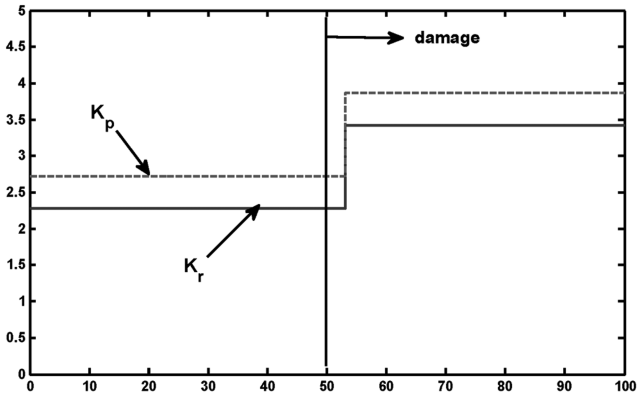

Fig. 25 K_p and K_r time histories for tracking of Fig. 24.

for $t > 125$ s. Stability was not affected. The increased error could be accommodated by the pilot incorporating low-frequency integration of the position error signal, a model modification beyond the scope of the present study. Figure 27 shows that this modification reduced the large crossover frequency for this system from 6.6 to 3 rad/s. This is still larger than the crossover frequencies of the remaining two controlled elements (as it should be) but more reasonable for this controlled element.

Pilot model adaptation in multiple-loop closures in single- or multi-axis tasks should pose no insurmountable difficulty. Multiple-loop closures means using outer-loop response variables to provide commands to inner loops through the same cockpit inceptor. For example, in modeling the pilot controlling a hovering helicopter, outer-loop longitudinal position errors provide commands for a longitudinal velocity control loop, and longitudinal velocity errors provide commands for an inner pitch attitude loop (s) (attitude and rate as per Fig. 1), which is then controlled through longitudinal cyclic inputs by the pilot. Given the structure of the pilot model as presented in [19], as one moves from the innermost rate loop to the outer control loops, the necessity of adaptation decreases sharply.

Use of the pilot model for gradual change in controlled element dynamics also appears feasible. Although only a single example is considered for such cases, the ability of the same model structure as used in the previous examples to accommodate these gradual changes is encouraging.

It must be emphasized that the adaptive model developed herein cannot be considered to be in its final form. It can, however, serve as a point of departure for studying human pilot control behavior in a variety of tasks in which vehicle dynamics change in unpredictable fashion. Quoting from [27] published over four decades ago, this modeling approach is simply offered as a tool that has the potential "...to summarize behavioral data, to provide a basis for rationalization and understanding of pilot control actions, and, most important of all, to be used in conjunction with vehicle dynamics in

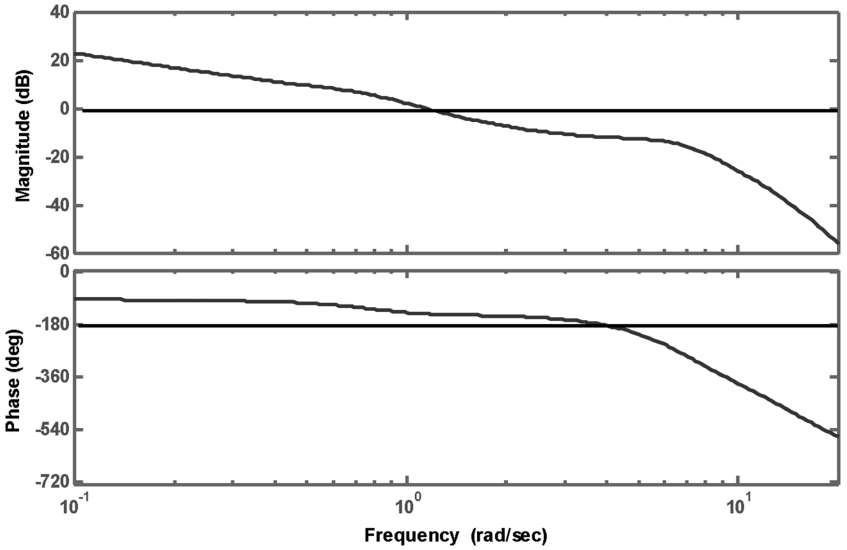

Fig. 26 Pilot/vehicle dynamics after adaptation.

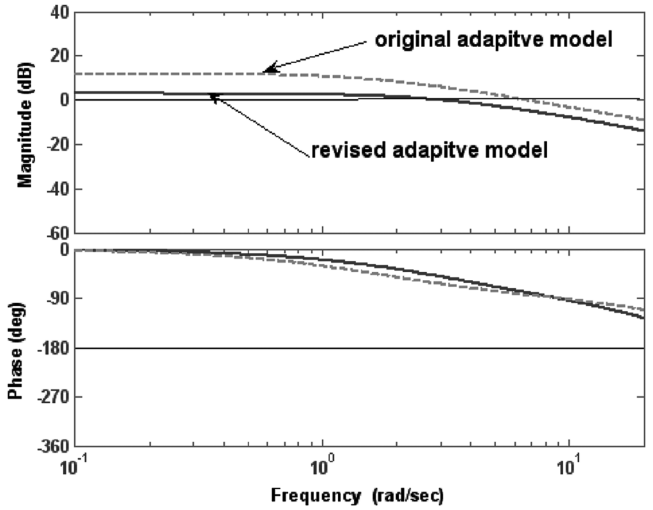

Fig. 27 Comparison of the bode plots of the open-loop pilot/vehicle transfer function for $Y_c = 1/(s + 50)$ after transition from $Y_c = 1/[s(s + 10)]$.

forming predictions or in explaining behavior of pilot-vehicle systems."

Conclusions

Based upon the preliminary research reported herein, the following conclusions can be drawn:

1) A model of the human pilot adapting to sudden changes in vehicle dynamics has been proposed and exercised using controlled elements that demand a wide range of pilot equalization as interpreted by the crossover model of the human pilot.

2) The nominal pilot model is based upon a simple two-loop pursuit structure previously introduced in the literature.

3) The adaptation logic meets four criteria:

a) Only signals that may be easily sensed by the human are employed.

b) The logic driving the adaptation must be simple.

c) Postadaptation pilot models follow the dictates of the crossover model of the human pilot.

d) Adaptation times are on the order of 5 s for sudden changes in controlled element dynamics.

4) It may be possible to employ the model in realistic, multi-axis, multiloop flight control tasks by employing separate pilot model structures in each axis subject to pilot control. The model also appears to be applicable to cases in which controlled element dynamics are subject to gradual, rather than sudden changes.

5) The structure of the pursuit model, emphasizing sequential loop closures, suggests that pilot model adaptation may be limited to the two innermost loops for any axis of control in multi-axis tasks.

6) The model provides a control-theoretic framework with which to study pilot control behavior in instances in which vehicle dynamics are subject to sudden, unpredictable changes.

Acknowledgment

The research reported herein was supported by a Cooperative Agreement with NASA Ames Research Center, funded under the NASA Subsonic Rotary Wing Project. Barbara Sweet serves as the grant technical manager.

References

[1] Krendel, E. S., and McRuer, D. T., "A Servomechanisms Approach to Skill Development," *Journal of the Franklin Institute*, Vol. 269, No. 1, 1960, pp. 24–42. doi:10.1016/0016-0032(60)90245-3

[2] Smith, R. H., "On the Limits of Manual Control," *IEEE Transactions on Human Factors in Electronics*, Vol. HFE-4, No. 1, 1963, pp. 56–59. doi:10.1109/THFE.1963.231287

[3] Hess, R. A., "The Human Operator as an Element in a Control System with Time Varying Dynamics," U.S. Air Force Flight Dynamics Lab, AFFDL-FDCC-TM-65-34, 1965.

[4] Elkind, J. I., and Miller, D. C., "Process of Adaptation by the Human Controller," *Proceedings of the Second Annual NASA-University Conference on Manual Control*, SP-128, NASA, 1966, pp. 47–63.

[5] Weir, D. H., and Phatak, A. V., "Model of Human-Operator Response to Step Transitions in Controlled Element Dynamics," *Proceedings of the Second Annual NASA-University Conference on Manual Control*, SP-128, NASA, 1966, pp. 65–83.

[6] Gould, E. E., and Fu, K. S., "Adaptive Model of the Human Operator in a Time-Varying Control Task," *Proceedings of the Second Annual NASA-University Conference on Manual Control*, SP-128, NASA, 1966, pp. 85–97.

[7] Li, Y. T., "Man in an Adaptive and Multiloop Control System," *Proceedings of the Second Annual NASA-University Conference on Manual Control*, SP-128, NASA, 1966, pp. 99–105.

[8] Weir, D. H., and Johnston, W. A., "Pilot's Response to Stability Augmentation System Failures and Implications for Design," *Proceedings of the Fourth Annual NASA-University Conference on Manual Control*, SP-192, NASA, 1968, pp. 341–360.

[9] Phatak, A. V., and Bekey, G. A., "Model of the Adaptive Behavior of the Human Operator in Response to a Sudden Change in the Control Situation," *Proceedings of the Fourth Annual NASA-University Conference on Manual Control*, SP-192, NASA, 1968, pp. 361–381.

[10] Weir, D. H., "Applications of the Pilot Transition Response Model to Flight Control System Failure Analysis," *Proceedings of the Fourth Annual NASA-University Conference on Manual Control*, SP-192, NASA, 1968, pp. 457–459.

[11] Preyss, A. E., and Meiry, J. L., "Stochastic Modeling of Human Learning Behavior," *IEEE Transactions on Man-Machine Systems*, Vol. MMS-9, No. 2, 1968, pp. 36–46. doi:10.1109/TMMS.1968.300006

[12] Phatak, A. V., and Bekey, G. A., "Decision Processes in the Adaptive Behavior of Human Controllers," *Proceedings of the Fifth Annual NASA-University Conference on Manual Control*, SP-215, NASA, 1969, pp. 429–451.

[13] Young, L. R., "On Adaptive Manual Control," *Ergonomics*, Vol. 12, No. 4, 1969, pp. 635–675. doi:10.1080/00140136908931083

[14] Gilstead, D. W., and Fu, K. S., "A Two Dimensional, Pattern Recognizing, Adaptive Model of a Human Controller," *Proceedings of the Sixth Annual Conference on Manual Control*, NASA, 1970, pp. 553–569.

[15] Delp, P., and Crossman, E. R. F. W., "Transfer Characteristics of Human Adaptive Response to Time-Varying Dynamics," *Proceedings of the Eighth Annual Conference on Manual Control*, NASA, 1972, pp. 245–271.

[16] Niemela, R. J., and Krendel, E. S., "Detection of a Change in Plant Dynamics in a Man-Machine System," *Proceedings of the Tenth Annual Conference on Manual Control*, NASA, 1974, pp. 97–111.

[17] Curry, R. E., and Govindaraj, T., "The Human as a Detector of Changes in Variance and Bandwidth," *Proceedings of the Thirteenth Annual Conference on Manual Control*, NASA, 1977, pp. 217–221.

[18] Steinberg, M., "Historical Overview of Research in Reconfigurable Flight Control, Proceedings of the Institution of Mechanical Engineers," *Journal of Aerospace Engineering*, Vol. 219, No. G4, 2005, pp. 263–276.

[19] Hess, R. A., "Simplified Approach for Modelling Pilot Pursuit Control Behaviour in Multi-Loop Flight Control Tasks, Proceedings of the Institution of Mechanical Engineers," *Journal of Aerospace Engineering*, Vol. 220, No. G2, 2006, pp. 85–102.

[20] McRuer, D. T., and Krendel, E. S., "Mathematical Models of Human Pilot Behavior," AGARDograph No. 188, 1974.

[21] Hess, R. A., "Obtaining Multi-Loop Pursuit-Control Pilot Models from Computer Simulation, Proceedings of the Institution of Mechanical Engineers," *Journal of Aerospace Engineering*, Vol. 222, No. G2, 2008, pp. 189–199.

[22] Hess, R. A., "Structural Model of the Adaptive Human Pilot," *Journal of Guidance and Control*, Vol. 3, No. 5, 1980, pp. 416–423. doi:10.2514/3.56015

[23] Kleinman, D. L., Baron, S., and Levison, W. H., "An Optimal Control Model of Human Behavior," *Proceedings of the Fifth Annual NASA-University Conference on Manual Control*, NASA, SP-215, 1969.

[24] Hess, R. A., "Feedback Control Models—Manual Control and Tracking," *Handbook of Human Factors and Ergonomics*, edited by G. Salvendy, Wiley, New York, 1997, Chap. 38.

[25] Hess, R. A., and Marchesi, F., "Pilot Modeling with Applications to the Analytical Assessment of Flight Simulator Fidelity," *Journal of Guidance, Control, and Dynamics*, Vol. 32, No. 3, 2009, pp. 760–770. doi:10.2514/1.40645

[26] Hess, R. A., and Wells, S. R., "Sliding Mode Control Applied to Reconfigurable Flight Control Design," *Journal of Guidance, Control, and Dynamics*, Vol. 26, No. 3, 2003, pp. 452–462. doi:10.2514/2.5083

[27] McRuer, D. T., and Jex, H. R., "A Review of Quasi-Linear Pilot Models," *IEEE Transactions on Human Factors in Electronics*, Vol. HFE-8, No. 3, 1967, pp. 181–249. doi:10.1109/THFE.1967.233967